Elastic differential cross section at 7 TeV and dynamical gluon mass model predictions

D. A. Fagundes[1], E. G. S. Luna[2], M. J. Menon[1], A. A. Natale[3]

[1]IFGW - UNICAMP
[2]IF - UFRGS
[3]IFT - UNESP

September 21, 2011

II Workshop on Diffractive Physics at the LHC

Outline

From ISR to LHC: $\sqrt{s} \sim 100\ \sqrt{s}_{ISR}$ and momentum transfer up to 10 GeV^2 $\rightarrow$ huge experimental developments

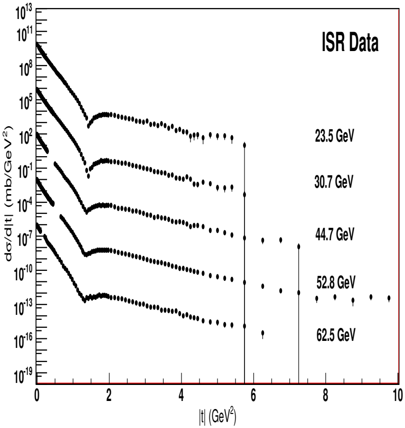

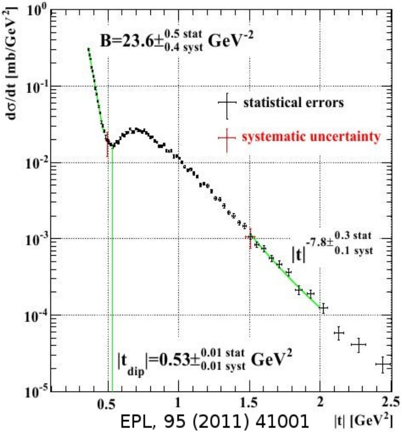

Good moment for testing model predictions!

DGM Approach - Partons and Minijet Cross Section

The rise of σ_{jet} (s) is driven by low-x parton-parton collisions.
From the Parton Model, the perturbative jet cross section follows

$$\begin{aligned} \sigma^{AB}_{jet}(s, p_{tmin}) &= \mathcal{D}(s, p_{tmin}) \left\{ \sum_{i,j,k,l} f_{i|A}(x_1, p_t^2) f_{j|B}(x_2, p_t^2) \frac{d\hat{\sigma}^{kl}_{ij}(\hat{s})}{dp_t} \right\} \\ \mathcal{D}(s, p_{tmin}) &\equiv \int_{p_{tmin}}^{\sqrt{s}/2} dp_t \int_{4p^2_{tmin}/s}^{1} dx_1 \int_{4p^2_{tmin}/(x_1 s)}^{1} dx_2 \qquad (1) \end{aligned}$$

x_1, x_2 the fractions of particle momentum carried by partons,
$\sqrt{\hat{s}} = \sqrt{x_1 x_2 s}$ the CM energy of two partons and $\hat{\sigma}$ the hard parton cross section

DGM Approach - Rise of gg Interactions

Ansatz: the gluon distribution function inside the colliding hadrons grow with the energy and is the main responsable for the rise of $\sigma_{jet}^{AB}(s)$. Perturbative QCD gives us the $gg \to gg$ cross section:

$$\frac{d\hat{\sigma}}{d\hat{t}}(\hat{s},\hat{t}) \quad = \quad \frac{9\pi\alpha_s^2}{2\hat{s}}\left\{3+\frac{\hat{s}[\hat{s}+\hat{t}]}{\hat{t}^2}+\frac{\hat{s}\hat{t}}{[\hat{s}+\hat{t}]^2}+\frac{\hat{t}[\hat{s}+\hat{t}]}{\hat{s}^2}\right\}$$

which we know to be valid only for high-p$_t$! How to connect with the IR region?!

$$\downarrow$$

Solutions of Schwinger-Dyson Equations (SDE)

$$+$$

Dynamical Perturbation Theory

DGM Approach - Dynamical Perturbation Theory

Main ideia: to recover the perturbative limit when $\hat{s} \gg \Lambda_{QCD}$.
From DPT follows the elementary cross section $gg \to gg$

$$\frac{d\hat{\sigma}^{DPT}}{d\hat{t}}(\hat{s},\hat{t}) = \frac{9\pi\bar{\alpha}_s^2}{2\hat{s}}\left\{3 - \frac{\hat{s}[4M_g^2(\hat{s}) - \hat{s} - \hat{t}]}{[\hat{t} - M_g^2(\hat{s})]^2} - \frac{\hat{s}\hat{t}}{[3M_g^2(\hat{s}) - \hat{s} - \hat{t}]^2} - \frac{\hat{t}[4M_g^2(\hat{s}) - \hat{s} - \hat{t}]}{[\hat{s} - M_g^2(\hat{s})]^2}\right\} \quad (2)$$

where $\bar{\alpha}_s$ and M_g are Cornwall's finite coupling constant and dynamical gluon mass.

From Cornwall's solution of SDE for the gluon propagator, the frozen coupling constant arises

$$\bar{\alpha}_s(\hat{s}) = \frac{4\pi}{\beta_0 \ln\left[(\hat{s} + 4M_g^2(\hat{s}))/\Lambda^2\right]}, \quad (3)$$

and the dynamical gluon mass

$$M_g^2(\hat{s}) = m_g^2 \left[\frac{\ln\left(\frac{\hat{s}+4{m_g}^2}{\Lambda^2}\right)}{\ln\left(\frac{4m_g^2}{\Lambda^2}\right)}\right]^{-12/11}, \quad (4)$$

where $\beta_0 = 11 - \frac{2}{3}n_f$ (n_f is the number of flavors) and $\Lambda = \Lambda_{QCD}$.

DGM Approach - PQCD Limit

In the high-energy limit ($\hat{s} \gg \Lambda_{QCD}$)

$$M_g \to 0$$

$$\bar{\alpha}_s \to \alpha_s$$

$$\Downarrow$$

$$\frac{d\hat{\sigma}}{d\hat{t}}(\hat{s},\hat{t}) \quad \to \quad \frac{9\pi\alpha_s^2}{2\hat{s}}\left\{3 + \frac{\hat{s}[\hat{s}+\hat{t}]}{\hat{t}^2} + \frac{\hat{s}\hat{t}}{[\hat{s}+\hat{t}]^2} + \frac{\hat{t}[\hat{s}+\hat{t}]}{\hat{s}^2}\right\}$$

PQCD result recovered!!

Using this fact, we have studied high-energy elastic scattering in an eikonalized framework.

Scattering Amplitude

The elastic amplitude is written as

$$A(s,t) = i \int b db J_0(qb)[1 - \mathrm{e}^{i\chi(s,b)}], \tag{5}$$

$s, q^2 = -t$ are the Mandelstam variables

Even and Odd Eikonals

For the two channels analyzed we have the complex eikonal function

$$\chi_{pp}^{\bar{p}p}(s,b) = \chi^{+}(s,b) \pm \chi^{-}(s,b) \tag{6}$$

where $\chi^{\pm}$ are the even/odd under crossing eikonals.

Physical Observables

All the observables are written in terms of the complex eikonal function

$$\sigma_{tot}(s) = 4\pi \int_0^\infty b\, db\, [1 - e^{-\chi_I(b,s)} \cos \chi_R(b,s)], \quad (7)$$

$$\sigma_{el}(s) = 2\pi \int_0^\infty b\, db\, |1 - e^{i\chi(b,s)}|^2, \quad (8)$$

$$\sigma_{in}(s) = 2\pi \int_0^\infty b\, db\, [1 - e^{-2\chi_I(b,s)}], \quad (9)$$

$$\rho(s) = \frac{\mathrm{Re}\{i \int b\, db\, [1 - e^{i\chi(b,s)}]\}}{\mathrm{Im}\{i \int b\, db\, [1 - e^{i\chi(b,s)}]\}}, \quad (10)$$

$$\frac{d\sigma_{el}}{d|t|}(s,t) = \pi \left| \int b db J_0(qb)[1 - e^{i\chi(b,s)}]\right|^2. \quad (11)$$

Connection with Elementary Processes

Again, gluons of low-x dominate interactions at high energy, $\sqrt{s}$. The major contribution comes from the even part, parametrized as

$$\begin{aligned} \chi^{+}(b,s) &= \chi_{qq}(b,s) + \chi_{qg}(b,s) + \chi_{gg}(b,s) \\ &= i[\sigma_{qq}(s) W(b;\mu_{qq}) + \sigma_{qg}(s) W(b;\mu_{qg}) \\ &+ \sigma_{gg}(s) W(b;\mu_{gg})]. \end{aligned} \tag{12}$$

The odd one accounts for the difference between channels pp and $\bar{p}p$ at low energy (*a la* Regge)

$$\chi^{-}(b,s) = C^{-} \Sigma \frac{m_g}{\sqrt{s}} e^{i\pi/4} W(b;\mu^{-}), \tag{13}$$

where $W(b,\mu_{ij})$, $ij = qq, qg, gg$, is the overlap function in b-space and σ_{ij} simulates interactions between quarks and gluons.

gg contribution

From the Parton Model, the expression for $\sigma_{gg}(s)$ follows

$$\sigma_{gg}(s) = C' \int_{4m_g^2/s}^{1} d\tau \, F_{gg}(\tau) \, \hat{\sigma}_{gg}(\hat{s}), \qquad (14)$$

where $F_{gg}(\tau)$ is the gluon distribution function,

$$F_{gg}(\tau) = [g \otimes g](\tau) = \int_{\tau}^{1} \frac{dx}{x} \, g(x) \, g\left(\frac{\tau}{x}\right), \qquad (15)$$

and $\hat{\sigma}_{gg}(\hat{s})$ represents the $gg \to gg$ nonperturbative cross section

$$\begin{aligned} \hat{\sigma}_{gg}(\hat{s}) &= \left(\frac{3\pi\bar{\alpha}_s^2}{\hat{s}}\right) \left\{ \frac{12\hat{s}^4 - 55M_g^2\hat{s}^3 + 12M_g^4\hat{s}^2 + 66M_g^6\hat{s} - 8M_g^8}{4M_g^2\hat{s}[\hat{s} - M_g^2]^2} \right. \\ &- \left. \left[3\ln\left(\frac{\hat{s} - 3M_g^2}{M_g^2}\right) \right] \right\} . \end{aligned} \qquad (16)$$

We have considered the instrumental gluon distribution function

$$g(x) = N_g \, \frac{(1-x)^5}{x^J}, \tag{17}$$

where $J = 1 + \epsilon$ and ϵ is the soft Pomeron intercept. Then assymptotically σ_{gg} goes like:

$$\lim_{s\to\infty} \int_{4m_g^2/s}^{1} d\tau \, F_{gg}(\tau) \, \hat{\sigma}_{gg}(\hat{s}) \sim \left(\frac{s}{4m_g^2}\right)^{\epsilon} \ln\left(\frac{s}{4m_g^2}\right). \tag{18}$$

Therefore, ϵ and m_g influences extrapolations to higher energies and cannot be arbitrarily fixed.

Elementary Cross Sections

qq and qg contribution

Motivation: from the instrumental distribution function at low-x

$$q(x) = \frac{(1-x)^3}{\sqrt{x}}, \tag{19}$$

it follows the qq and qg cross sections

$$\sigma_{qq}(s) = \Sigma A \frac{m_g}{\sqrt{s}} \to \text{Regge-like} \tag{20}$$

$$\sigma_{qg}(s) = \Sigma \left[A' + B' \ln\left(\frac{s}{m_g^2}\right)\right] \to \text{Log-like.} \tag{21}$$

which we understand to dominate at low and intermediate $\sqrt{s}$.

Fit Procedure and Results

Fits to the experimental data $\sigma_{tot}(s)$, $\rho(s)$ and $\frac{d\sigma_{el}^{\bar{p}p}}{d|t|}$(546 GeV and 1.80 TeV) with CL 90% using *TMinuit Class - ROOT*

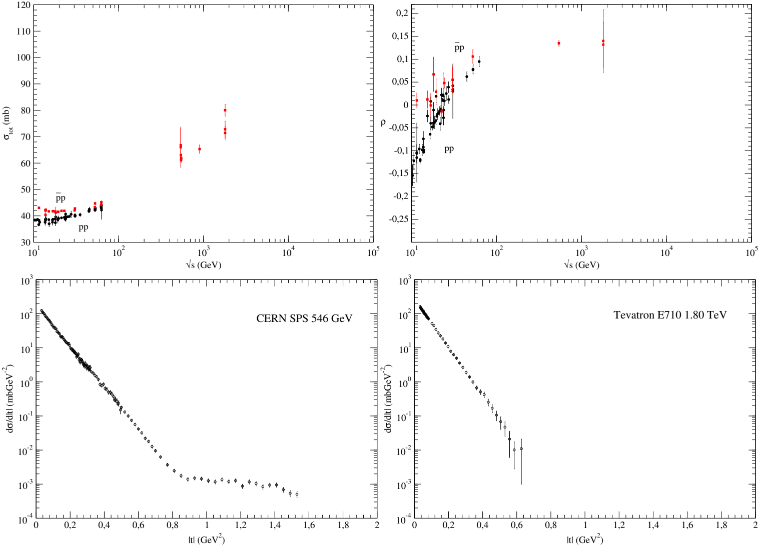

Testing Parameters

We have tested a set of values for the mass m_g and for the P intercept, ϵ:

$$m_g = 350,\ 400,\ 450 \text{ and } 500 \text{ MeV}$$

and

$$\epsilon = 0.080,\ 0.085 \text{ and } 0.090$$

Next it follows the results with $\epsilon = 0.080$.

Fit Results - $\sigma_{tot}(s)$ and $\rho(s)$

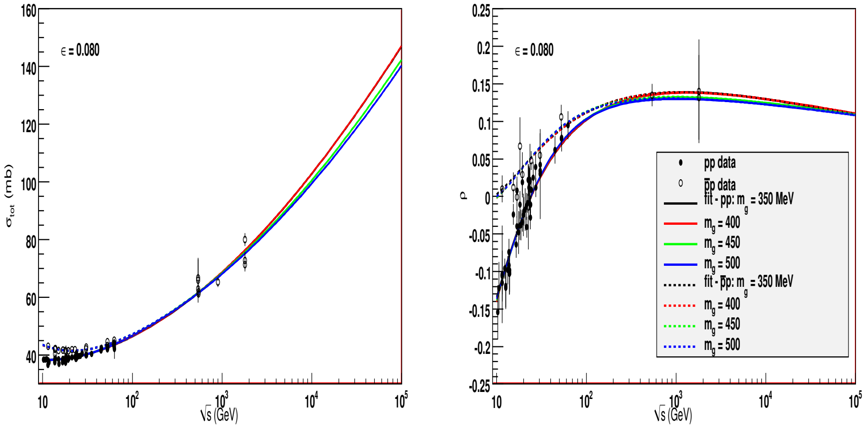

Fit Results - $\frac{d\sigma_{el}^{\bar{p}p}}{d|t|}$ (546 GeV and 1.80 TeV)

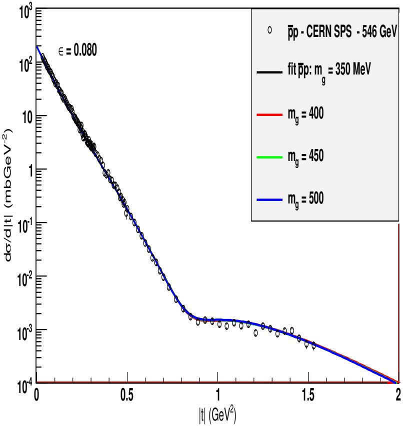

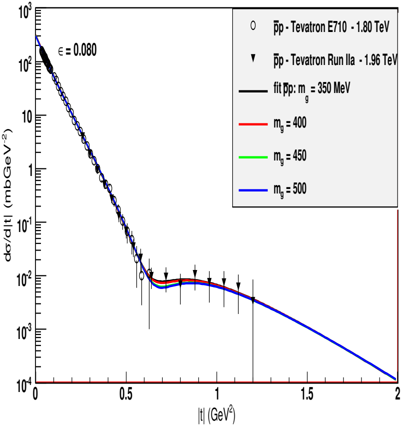

Predictions - $\frac{d\sigma_{el}^{pp}}{d|t|}$ e slope B(t) 7.0 TeV

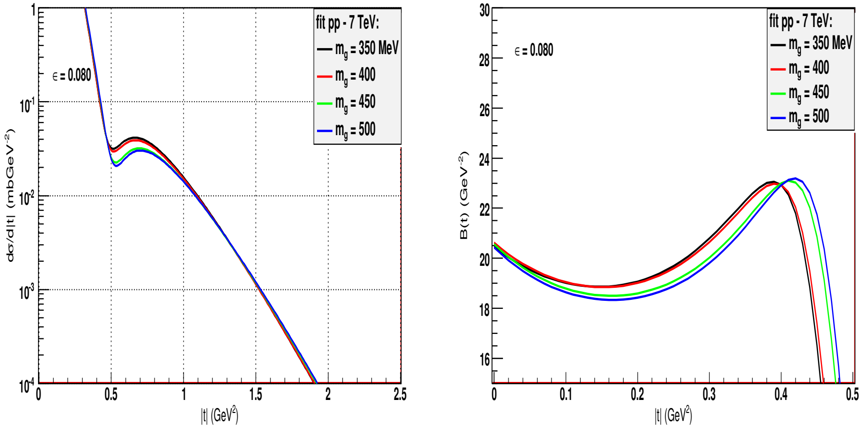

Fit Results - Variations of m_g

m_g [MeV]	$B(\lvert t\rvert=0.4\ \mathrm{GeV}^2)$ [GeV^{-2}]	$\lvert t_{dip}\rvert$ [GeV^2]	n in $\lvert t\rvert^{-n}$ [$1.5 \leq \lvert t\rvert \leq 2.0\ \mathrm{GeV}^2$]	$d\sigma/dt$ ($\lvert t\rvert=0.7\ \mathrm{GeV}^2$) [$\mathrm{mb}/\mathrm{GeV}^2$]
350	22.9	0.51	10.6	4.1×10^{-2}
400	22.9	0.52	10.5	3.8×10^{-2}
450	23.0	0.53	10.3	3.2×10^{-2}
500	22.9	0.54	10.2	3.0×10^{-2}
Mean Value	22.9 ± 0.05	0.53 ± 0.01	10.4 ± 0.2	$(3.5\pm0.5)\times10^{-2}$

Predictions - Comparison with TOTEM's Measurement and Other Models

Experiment and Theory	$B_{(\lvert t \rvert=0.4\ \mathrm{GeV}^2)}$ [GeV^{-2}]	$\lvert t_{dip} \rvert$ [GeV^2]
TOTEM Measurement	23.6 $\pm 0.5^{stat} \pm 0.4^{sys}$	0.53 $\pm 0.01^{stat} \pm 0.01^{sys}$
Block *et al.*	24.4	0.48
Bourrely *et al.*	21.7	0.54
Islam *et al.*	19.9	0.65
Jenkovszki *et al.*	20.1	0.72
Petrov *et al.*	22.7	0.52
DGM	22.9±0.05	0.53±0.01

Predictions - Comparison with TOTEM's Measurement and Other Models

Experiment and Theory	n in $\lvert t\rvert^{-n}$ [$1.5 \leq \lvert t\rvert \leq 2.0$ GeV^2]	$d\sigma/dt$ ($\lvert t\rvert=0.7$ GeV^2) [mb/GeV^2]
TOTEM Measurement	7.8 $\pm 0.3^{stat} \pm 0.1^{sys}$	2.7×10^{-2} $+3.7\%^{stat}\ {}^{+26\% syst}_{-21\% syst}$
Block *et al.*	10.4	9.1×10^{-2}
Bourrely *et al.*	8.4	4.8×10^{-2}
Islam *et al.*	5.0	8.2×10^{-3}
Jenkovszki *et al.*	4.2	6.1×10^{-3}
Petrov *et al.*	7.0	4.2×10^{-2}
DGM	10.4 ± 0.2	$(3.5\pm0.5)\times10^{-2}$

Fit Procedure and Results

Predictions - $\frac{d\sigma_{el}^{pp}}{d|t|}$ 7.0 TeV

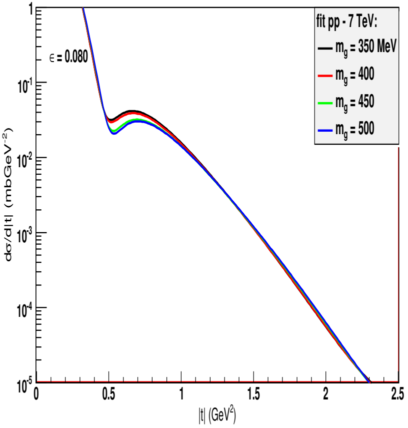

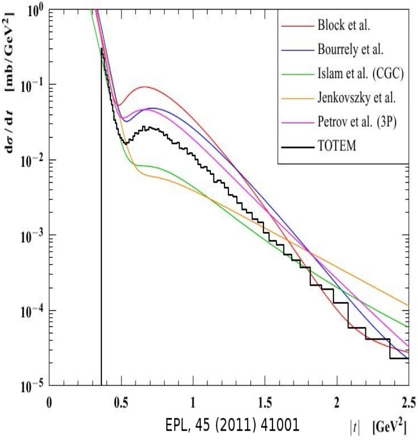

Predictions to LHC and Auger

m_g (MeV):	350	400	450	500	Mean Value
σ_{tot} (7 TeV) (mb)	96.9	96.9	94.9	94.0	95.7±1.5
σ_{tot} (14 TeV) (mb)	108.8	108.8	106.1	104.9	107.2±2.0
σ_{tot} (57 TeV) (mb)	135.4	135.6	131.3	129.5	133.0±3.0
σ_{in} (7 TeV) (mb)	72.2	72.3	71.2	70.6	71.58±0.82
σ_{in} (14 TeV) (mb)	79.6	79.8	78.3	77.5	78.8±1.1
σ_{in} (57 TeV) (mb)	95.8	96.1	93.9	92.8	94.7±1.6
σ_{el}/σ_{tot} (7 TeV)	0.255	0.254	0.250	0.249	0.2520±0.0029
σ_{el}/σ_{tot} (14 TeV)	0.268	0.266	0.262	0.261	0.2643±0.0033
σ_{el}/σ_{tot} (57 TeV)	0.292	0.291	0.285	0.283	0.2878±0.0044

Summary and Outlook

- Good statistical description of all analyzed data (pp and $\bar{p}p$)
- Dif. Cross Sec. at 7 TeV $\rightarrow$ best results with $\epsilon = 0.080$ and $m_g = 450 - 500$ MeV
- Competitive approach (among representatives)
- First explicity connection with NPQCD (as expected at small t region)

Next Steps

- New tests on gluon distribution functions (CTEQ, MRST, MSTW) and form factors
- Extensions to other channels: meson-p, gamma-p and gamma-gamma
- Inelastic channel (unitarity)

Acknowledgements

This work is support by

Thank you!!!